Published in final edited form as:
Ann Biomed Eng. 2011 August ; 39(8): 2242–2251. doi:10.1007/s10439-011-0323-4.

Rapid Microfluidic Perfusion Enabling Kinetic Studies of Lipid Ion Channels in a Bilayer Lipid Membrane Chip

Chenren Shao[1], **Bing Sun**[2], **Marco Colombini**[2], and **Don L. DeVoe**[3]

[1]Department of Mechanical Engineering, University of Maryland, 3123 Glenn L Martin Hall, College Park, MD 20742, USA

[2]Department of Biology, University of Maryland, College Park, MD, USA

[3]Department of Mechanical Engineering, University of Maryland, 3139 Glenn L Martin Hall, College Park, MD 20742, USA

Abstract

There is growing recognition that lipids play key roles in ion channel physiology, both through the dynamic formation and dissolution of lipid ion channels and by indirect regulation of protein ion channels. Because existing technologies cannot rapidly modulate the local (bio)chemical conditions at artificial bilayer lipid membranes used in ion channel studies, the ability to elucidate the dynamics of these lipid–lipid and lipid–protein interactions has been limited. Here we demonstrate a microfluidic system supporting exceptionally rapid perfusion of reagents to an on-chip bilayer lipid membrane, enabling the responses of lipid ion channels to dynamic changes in membrane boundary conditions to be probed. The thermoplastic microfluidic system allows initial perfusion of reagents to the membrane in less than 1 s, and enables kinetic behaviors with time constants below 10 s to be directly measured. Application of the platform is demonstrated toward kinetic studies of ceramide, a biologically important lipid known to self-assemble into transmembrane ion channels, in response to dynamic treatments of small ions (La^{3+}) and proteins (Bcl-x_L mutant). The results reveal the broader potential of the technology for studies of membrane biophysics, including lipid ion channel dynamics, lipid–protein interactions, and the regulation of protein ion channels by lipid micro domains.

Keywords

Bilayer lipid membrane; Ceramide; Ion channels; Protein-lipid interactions

INTRODUCTION

Studies of protein ion channels commonly treat the lipid membrane as a simple inert supporting layer. However, it is now widely recognized that lipids themselves play important biological roles as direct signaling elements[35,42] and protein ion channel regulators.[13,14] A wide range of protein ion channels have been shown to associate with lipid micro domains,[41] with regulation of channel conductance resulting from interactions with the lipids as well as changes in the physical properties of the membrane.[12] Moreover, lipids can self organize into stable pore structures,[34,36] resulting in ion channels that display quantized conductance states with similar lifetimes and magnitudes as protein ion

Address correspondence to Don L. DeVoe, Department of Mechanical Engineering, University of Maryland, 3139 Glenn L Martin Hall, College Park, MD 20742, USA. ddev@umd.edu.

channels.[2,6,29,30,59] Just like protein ion channels, lipid channels also respond to external stimuli such as temperature, pH,[53] voltage,[3] lateral tension,[21] and chemicals.[22]

The sphingolipid ceramide is a particularly interesting example of a lipid ion channel proposed to play a decision making role in apoptotic programmed cell death. In the early stage of apoptosis, increased ceramide concentration precedes mitochondrial outer membrane (MOM) permeabilization and the release of intermembrane space proteins including apoptosis-inducing factors.[4,11,31,33,49] The mechanistic relationship between elevated ceramide concentration and MOM permeability has been investigated using an analytical structural model[43] and by molecular dynamics simulations,[1] with experimental support provided by electrophysiological measurements,[19,43–45,47] isolated mitochondrial assays,[19,45,47,48] and comparison of ceramide and its dihydroceramide analogs.[46] It is believed that ceramide forms stable channel structures with ohmic behavior,[18,43] in which the amide and carbonyl groups of ceramide form stable intermolecular hydrogen bonds, resulting in columnar ceramide structures that further inter-connect by hydrogen bonding and form a transmembrane nanopore with hydrophilic ceramide heads oriented toward the membrane core.[44] In contrast to protein ion channels, ceramide channels can exhibit dramatic pore size changes in response to different physiological conditions, with discrete conductance jumps due to channel enlargement or shrinkage rather than gating behavior across a population of channels.[44] Despite compelling evidence for this ceramide channel model, there is limited knowledge on the kinetics of ceramide recruitment and dispersion in response to dynamic changes in chemical boundary conditions. Indeed, most existing observations of both lipid channels and lipid–protein interactions are based on measurements with static chemical boundary conditions.[12] The time scale of these dynamics is on the order of tens of seconds,[10] significantly slower than channel gating exhibited by protein ion channels, but far too fast for traditional bilayer lipidmembrane (BLM)systems. While reagents can be added to traditional BLM systems by manual or automated pipetting, milliliter chamber volumes preclude the controllable delivery of precise time-dependent solute concentrations to the membrane. Moreover, the large diffusive length scales involved prohibit the delivery of steep gradients to the membrane, making it impossible to deconvolute the responses due to the bulk perfusion gradients and dynamic events within the membrane. Similarly, rapid removal of reagents introduced to the fluid surrounding the membrane is not feasible, such that responses to cyclic inputs cannot be readily determined. Furthermore, large-volume buffer exchange requires a careful balance of inflow and outflow to avoid membrane rupture due to hydraulic pressure disturbances, and often require multiple pumping cycles to complete the exchange.[28] Because buffer exchange as currently practiced is slow, delicate, and irreproducible, with the local concentration of reagents at the membrane site unknown at any given time point, this technique is not suitable for studying the dynamics associated with lipid–lipid or lipid–protein interactions in response to external modulation of the chemical boundary conditions using a bilayer membrane model.

An alternative to bulk perfusion systems is to leverage the small volumes inherent to microfluidics technology to achieve rapid and controllable perfusion of solutes to an on-chip bilayer lipid membrane. Despite significant overall advances in microfluidic BLM platforms,[15–17,25,32,37–39,50,51] a practical system for dynamic ion channel measurements in the presence of well-defined time-varying chemical inputs remains elusive. Existing microfluidic systems rely on diffusive transport, either by directly depositing reagents into an open chamber in fluidic contact with the membrane, or through an interconnecting microchannel. For example, Suzuki *et al.*[51] pipetted gramicidin into a reservoir connected to a channel positioned below the bilayer membrane, with diffusion leading to incorporation of gramicidin into the bilayers. In an alternate approach, Hromada *et al.*[25] studied the interaction between poly(ethylene glycol) (PEG) with alpha-hemolysin ion channels by pre-

filling a channel with PEG solution before forming the membrane through an open well above the channel.

The long time scales associated with diffusion transport preclude the implementation of high-frequency dynamic studies. More generally, diffusion does not allow for precise time-varying control of reagent concentration at the ion channel sites, enable specific time courses of chemical inputs with both increasing and decreasing concentrations, or provide a means for modulating the concentrations of multiple reagents. Thus the ability to rapidly perfuse chemicals to membrane-bound channels by pressure-driven convective transport would open the door to a wide range of ion channel studies which are not presently feasible.

Here we demonstrate rapid perfusion in a thermoplastic microfluidic chip to investigate the response of ceramide ion channels under the application of time-varying chemical concentrations. The microfluidic system minimizes pressure gradients across the bilayer membranes during perfusion, enabling rapid pumping of reagents to the ion channel sites without disrupting the fragile membranes. The BLMs are formed in an open well using a diffusive painting method reported by our group previously,[25] with delivery of reagents to the membrane sites performed through a microchannel positioned on the lower side of the membrane. The geometry of the channel downstream of the membrane is designed to minimize hydraulic resistance and backside pressure on the membrane during perfusion, while a simple wax sealing method employed at the electrode interfaces serves to reduce pressure variations within the fluidic system. The microfluidic chip is found to support volumetric flow rates above 10 μL/min for continuous perfusion, and significantly higher flow rates up to 20 μL/min for rapid pulse injection of reagent plugs, enabling perfused reagents to reach the membrane in less than 1 s and allowing steady-state concentrations to be defined under 10 s.

Performance of the microfluidic perfusion system is explored through the first demonstrated measurements of kinetics associated with formation, growth, and disassembly of ceramide ion channels in response to defined chemical inputs. Ceramide channels are shown to be inhibited by La^{3+}, with rapid reversal upon the injection of ethylenediaminetetraacetic acid (EDTA). Similarly, kinetic interactions between ceramide channels and Bcl-x_L Y101K mutant are evaluated, together with the dynamics of channel inhibition upon removal of Bcl-x_L mutant from the membrane site.

MATERIALS AND METHODS

Reagents

N-Hexadecyl-D-*erythro*-sphingosine (C_{16}-ceramide), asolectin (soybean phospholipids), 1,2-dipalmitoyl-*sn*-glycero-3-phosphocholine (DPPC), and cholesterol were purchased from Avanti Polar Lipids (Alabaster, AL). 1-Hexanol, *n*-hexadecane, ethylenediaminetetraacetic acid (EDTA), and piperazine-*N*,*N*′-bis(2-ethanesulfonic acid) (PIPES) were purchased from Sigma-Aldrich (St. Louis, MO). Bcl-x_L Y101K mutants were prepared following established procedures.[5,60]

Microfluidic System Fabrication

The microfluidic chip was fabricated from a multilayer assembly of thermoplastic materials (Fig. 1). Two polycarbonate (PC) wafers (2.38 mm thick, 8.9 cm diameter; McMaster-Carr, OH) were patterned by direct micromilling using a computer numerical control (CNC) machine. A 1.6 mm diameter hole was first drilled through the center of the upper PC wafer to serve as an open access well to the BLM site in the final chip, followed by the formation of two upper channels (460 μm wide, 120 μm deep) connecting the access well to independent inlet reservoirs. Two additional channel segments were milled in the upper

wafer, and a lower channel segment (150 μm wide, 120 μm deep) was micromilled in the bottom PC wafer such that the ends of the lower channel were positioned below the closed ends of each of the upper channel segments. A side channel with multiple inlets was connected to one of these channels, providing access for the independent introduction of different perfusion reagents. Inlet ports (0.65 mm diameter) and electrodes reservoirs (3.5 mm diameter) were drilled after channel fabrication, and machining debris were removed by ultra-sonication. The PC wafers were degassed at 100 °C in vacuum overnight and a layer of PVDC (12.5 μm thick; Sheffield Plastics, MA) was applied to the bottom wafer and temporarily held in place by van der Waals forces. A small aperture between 50 and 150 μm in diameter was formed through the PVDC film over the center of the lower channel by a hot needle attached to a probe station, while two additional holes were formed by the hot needle method to provide connections between the lower channel segment beneath the BLM site and the upper channel segments aligned to this lower channel. Smaller apertures allow the formation of lipid membranes with higher stability in the presence of transmembrane pressure gradients. The lower PC/PVDC substrate was thermally bonded in a hot press (Auto-Four/15, Carver, IA) at 141 °C and 70 kPa for 1 min. The upper PC was then carefully positioned over the bottom substrate to ensure alignment of the microchannel connections and BLM site access through the open well, and a final thermal bonding step was performed at 141 °C and 200 kPa for 10 min to form a permanent seal between the full PC/PVDC/PC assembly. As a low dead-volume world-to-chip interface, hypodermic stainless steel needle segments (2.54 mm long, 22 s gauge; Hamilton, Reno, UT) were inserted into the 650 μm diameter holes previously drilled through the upper PC wafer, providing convenient connections for off-chip MicroTight tubing (Upchurch, WA).[7]

Bulk Ag/AgCl electrodes were integrated into the fabricated chips for measurements of transmembrane current signals by inserting a sinter pellet wire electrode (A–M Systems, WA) into a NanoPort (Upchurch Scientific, WA) through a standard fitting sleeve. The electrode assemblies were sealed to the chip surface using a reversible adhesive wax (C11444 Center Softseal Tackiwax; Cenco Scientific, IL). The wax seal prevents leakage from the microfluidic channels while allowing the electrodes to be easily replaced after excessive polarization is observed, or removed from the chip for reuse. A schematic of the electrical pathway and perfusion pathway are shown in Fig. 1b. The devices exhibit a typical parasitic capacitance of 3 pF and series resistance of 200 kΩ when filled with 0.25 M KCl solution.

Electrophysiology Measurements

As shown in Fig. 1b, the Ag/AgCl electrodes were connected to computer through a custom headstage, a 60 Hz noise eliminator (Hum Bug; AutoMate Scientific, CA), filter (LPF-202A, f_c = 10 kHz; Warner Instruments, CT) and digitizer (Digidata 1322A; Axon, CA). Clampex 9 software (Molecular Devices, CA) was used to record input voltage and output current data at a 50 kHz sampling rate. A homemade signal generator was used to provide 0–100 mV DC voltages to the membrane. Syringe pumps (PHD 2000; Harvard Apparatus, MA) were used to deliver fluids to the needle inlets for perfusion test. The chips and headstage were positioned within a Faraday cage and located on a vibration isolation table to minimize external noise. Clampfit 9 software (Molecular Devices, CA) and MATLAB (MathWorks, MA) were used to analyze the collected data.

The lipid solution used for BLM formation comprised a mixture of 5 mg/mL DPPC, 5 mg/mL asolectin, and 0.5 mg/mL cholesterol in a base solvent as described below. To enable ceramide channel formation, C_{16}-ceramide was added to this BLM solution at 0.134 mg/mL, or a 1:50 molar fraction ratio with respect to the phospholipids. Unlike water-soluble protein ion channels such as α-hemolysin (α-HL), lipid ion channels cannot be introduced to the BLM through the aqueous buffer since the water-insoluble lipids can readily aggregate in

the buffer or become adsorbed on the microchannel walls. To avoid these issues in macro-scale electrophysiology measurements, alternate methods have been developed, such as proteoliposome fusion,[8,9,56–58,61] mixing of lipid components in a monolayer before formation of the final bilayer,[40,54] enhanced lipid solubility using the addition of fatty acid depleted BSA[48] or direct delivery of the ion channel lipids by a glass tip.[23,24] Here we employ a diffusive painting method[25] using the above-described solution of membrane lipids and ceramide. In this process, a 0.5 μL pretreatment solution consisting of lipids in hexane was first pipetted to the BLM site, followed by a gentle stream of nitrogen gas to fully dry the site. The pretreatment solution covers the rim of the aperture with a layer of phospholipid, which serves to facilitate the thinning process of bilayer formation after painting, presumably due to hydrophobization of the PVDC surface. After filling the microfluidic network and open well with aqueous buffer (1 M KCl, 1 mM $MgCl_2$, and 20 mM PIPES), the electrodes were secured to the chip with mounting wax. A lipid solution was prepared in a base solvent of hexanol and hexadecane (v/v 10:1), which served to speed the membrane thinning process through the diffusion of hexanol into the surrounding buffer. The tip (300–500 μm diameter) of a glass rod was dipped in the lipid solution, and gently brushed across the aperture in the PVDC film, leaving a plug of lipid solution within the aperture. Due to miscible nature of hexanol and water (solubility of 1-hexanol in water: 6 g/L), the hexanol rapidly diffuses into the aqueous buffer, leaving lipid in hexadecane on the PVDC film and leading to self-assembly of a bilayer lipid membrane across the aperture within 5 min. By monitoring the capacitance across the PVDC film during the BLM formation process using a 20 mV_{p-p} 250 Hz triangle wave applied to the on-chip electrodes, the presence of a bilayer can be readily confirmed.

A ceramide channel typically forms with stepwise jumps within several minutes after bilayer formation. The 1:50 ceramide:lipid molar ratio was chosen to ensure that the channel formation process takes place at a reasonable pace. At a higher ceramide concentration of 1:25, the channel commonly grows too rapidly and often ruptures the membrane, probably due to sudden recruitment of large ceramide aggregates. At a smaller ceramide ratio of 1:100, on the other hand, very slow ceramide channel growth is observed. Note that despite the different behaviors of ceramide channel formation dynamics observed at these different molar ratios, in each case the channels exhibit the same stepwise growth pattern.

RESULTS AND DISCUSSION

On-Chip Perfusion

In an ideal BLM perfusion system, high flow rates are desirable to enable rapid modulation of selected reagents at the on-chip ion channels. The achievable perfusion rate is primarily limited by the pressure resistance of the lipid membrane. To reduce the pressure gradient experienced across the membrane during diffusion, a relatively large (460 μm wide and 120 μm deep) and short (3 cm) channel was used between the BLM site and the downstream waste reservoir. Because the back pressure generated during pumping is proportional to the fourth power of the hydraulic radius of the channel and inversely proportional to the channel length, this design was found to support a wide range of flow rates while maintaining a stable lipid membrane.

In addition to the maximum pressure resistance of the membrane, the presence of a reservoir of excess lipid within the membrane annulus connecting the central bilayer to the supporting PVDC film aperture was found to be an important factor impacting the perfusion limits. As revealed in a membrane capacitance measurements shown in Fig. 2, disturbance of the membrane was negligible for flow rates up to 2.5 μL/min, with specific capacitance remaining nearly constant at 0.37 $\mu F/cm^2$, and direct optical observation of the membrane revealed that the bilayer diameter remained unchanged over this range of perfusion flows.

However, for flow rates above this level, the boundary of the bilayer was observed to expand toward the edge of the aperture together with a corresponding increase in membrane capacitance. This can be interpreted as a combination of membrane bulging and consequential annulus thinning, when lipids and solvent in the annulus was continuously pulled out of annulus and taken up by the bilayer. Indeed, halting the perfusion resulted in a rapid return to the initial capacitance level as lipid within the membrane was allowed to return to the annulus reservoir. However, for flow rates at or above 3.5 μL/min, continuous pumping eventually led to membrane rupture, with a maximum membrane burst capacitance of 280 pF (1.82 μF/cm^2). The pressure gradient across the membrane associated with the burst capacitance is found to be 1420 Pa, consistent with the pressure directly calculated from the given channel geometry and flow rate. For shorter perfusion cycles, however, the membrane was found to remain stable at significantly higher flow rates up to 20 μL/min.

Dynamic Switching Resolution

The ability of the chip to resolve kinetic responses of ion channels to changes in chemical boundary conditions is determined by the rate at which perfused solutes can be delivered to the BLM site. Because perfusion is performed by pressure-driven flow, it is necessary to consider the distribution of solutes due to the combination of convection and diffusion. If lateral diffusion is too slow, the parabolic flow field resulting from convective Poiseuille flow will generate a shallow temporal concentration gradient of solute at the membrane. To ensure that lateral diffusion is sufficiently rapid to produce a nearly uniform distribution of solute across the channel width, the Taylor condition[52] requires that:

$$\frac{a^2}{4\pi^2 D} \ll \frac{l}{u}, \quad \text{or } \frac{D}{u} \gg \frac{a^2}{4\pi^2 l} \tag{1}$$

where a is the channel height, D is the diffusion coefficient, l is the channel length between the perfusion inlet and BLM site, and u is the average fluid velocity. For the chip described here, a = 120 μm and l = 21 mm, so that $D/u \gg 1.74 \times 10^{-8}$ m. Using diffusion coefficients of 6.2×10^{-10} m^2/s for La^{3+} and 8.5×10^{-11} m^2/s for the Bcl-x_L mutant, the maximum average flow velocities that will yield nearly uniform reagent distributions across the channel width are found to be 35.7 and 4.89 mm/s for La^{3+} and Bcl-x_L mutant, respectively. For the channel geometry used in the BLM chip, these velocities correspond to volumetric flow rates around 118 μL/min for La^{3+} and 16 μL/min for Bcl-x_L mutant. By Taylor dispersion theory, the distribution of solutes for flow rates well below these limits can be reduced to a one-dimensional longitudinal diffusion problem, with a solute front moving at half the maximum velocity ($u_o = 3u/2$) of the convective flow, and a diffusive profile relative to this moving boundary defined by an effective diffusion coefficient of

$$D_{\text{eff}} = D + \frac{a^2 u^2}{192 D} \tag{2}$$

In this case, the relative concentration of solute at the BLM site a distance L from the injection point is given by

$$\frac{C}{C_0} = \frac{1}{2} erfc\left(\frac{L - u_o t/2}{2\sqrt{D_{\text{eff}} t}}\right) \tag{3}$$

Here we define the switching time (τ) as the time required for the solute concentration to change from 5 to 95% of the final value. Solving (3) for t_1 and t_2 when C/C_0 = 0.05 and 0.95, respectively, the switching time is determined as $\tau = t_2 - t_1$. With a steady-state

perfusion flow rate of 10 μL/min, the switching time is 24.3 and 8.0 s for Bcl-x_L and La^{3+}, respectively, and kinetic events with time constants slower than these limits can be effectively resolved. While 2.5 μL/min is a suitable flow rate for steady-state perfusion, significantly higher flow rates can be applied for short periods without disrupting the bilayer membrane as summarized in Fig. 2. For example, at the maximum flow rate of 20 μL/min explored in this work, perfused reagents first reach the BLM site within 800 ms, and the 95% switching time for La^{3+} is only 5.8 s.

Ceramide Channel Disassembly and Reassembly

Hydrogen bonding between ceramide molecules enables ceramide to link into a columnar chain spanning the thickness of the lipid membrane, which further repeats itself in a cylinder to form a transmembrane pore. The size of the resulting ceramide ion channel is determined by the dynamic equilibrium between ceramide molecules in the channel and free ceramide or ceramide aggregates within the lipid membrane. Dynamic interactions between a ceramide channel and other bio-active molecules within the membrane or in the adjacent solutions are known to affect the equilibrium state.[19,45] Understanding these dynamic interactions may provide insights into both the structure of ceramide channels and their roles in cell apoptosis.

One such case of interest is the interaction between inhibitor La^{3+} ions and ceramide channels. It has been shown that La^{3+} is an effective ceramide channel inhibitor through solvent-free BLM experiments, in which sufficient addition of La^{3+} has been observed to significantly reduce or eliminate ceramide channel conductance.[44] We have similarly observed that the addition of La^{3+} to a BLM formed in our microfluidic system by direct painting methods reduces ceramide conductance, but rarely eliminates the channel (data not shown). By understanding how La^{3+} inhibits ceramide channels, we may gain new knowledge about the mechanisms of ceramide channel formation. Here we demonstrate the inhibition of ceramide channels through the perfusion of La^{3+}, together with the perfusion of EDTA as a known La^{3+} chelator which allows for reformation of the channels. As shown in Fig. 3, a phospholipid membrane containing ceramide molecules was formed and maintained at zero conductance in the presence of 50 μMLa^{3+}. The arrival of EDTA perfused at 0.2 μL/min chelated the La^{3+} and promoted the formation of a ceramide channel. The stepwise fluctuations of the channel reveal the dynamic nature of the membrane/channel system as a result of the channel's continuous recruitment or loss of free ceramide molecules from the membrane. Because of the low flow rate, a perfusion time of ~14 min is required to initiate channel formation, which together with the 72 s switching time prevents kinetics of the process from being probed in this test.

To explore the mechanism of La^{3+} inhibition, the time dependence of both the La^{3+} inhibition and EDTA chelation processes must be investigated. It is plausible that ceramide molecules diffuse away from the channel after disassembly, decreasing the probability of spontaneous channel reformation with longer time intervals before EDTA perfusion. Figure 4 presents a perfusion test in which La^{3+} and EDTA are alternately perfused to the membrane using a flow rate of 20 μL/min to enable rapid transitions between the chemical boundary conditions. In the initial membrane, a ceramide channel formed with a stable conductance of ~320 nS. Perfusion of 50 μMLa^{3+} in base buffer partially disassembled the ceramide channel, reducing the conductance to ~40 nS. As EDTA (50 μM in base buffer) displaced La^{3+} within the perfusion channel, residual La^{3+} in the BLM was chelated and the channel conductance returned to ~300 nS. Following a second cycle of La^{3+} perfusion, the channel conductance was again reduced, but to a higher level than observed after the initial disassembly step. As before, the reintroduction of EDTA allowed the channel to reform and assumes a conductance similar to the initial baseline level.

Due to the high perfusion flow rate used in these tests, the switching times for both La^{3+} and EDTA were below 6 s, while the experimental conductance trace in Fig. 4 reveals transients that occur over time scales of 12–22 s for the case of channel disassembly upon the introduction of La^{3+}, and 25–55 s for channel reassembly following La^{3+} chelation. In this test, the time required to reform the channel appears to be correlated with the degree of disassembly. It is also notable that the disassembly process occurs in a rapid but stepwise process, while reassembly is nearly instantaneous following a short lag time. This latter observation stands in contrast to the case shown previously in Fig. 3, where ceramide channel assembly following a long period of incubation with La^{3+} is a relatively slow and step-wise process, suggesting that the reassembly shown in Fig. 4 involves the recruitment of ceramide rafts that have not had time to fully dissociate and diffuse far from the channel after La^{3+} inhibition.

Interactions Between Ceramide Channels and Bcl-x_L Y101K Mutants

Bcl-x_L, a potent apoptosis inhibitor, is found both in the cytosol and attached to mitochondrial membranes in healthy cells.[20,26] Overexpression of Bcl-x_L in the B lymphocyte cell line WEHI231 in known to protect against ceramide-induced apoptosis without altering the cellular level of ceramide.[55] By directly introducing Bcl-x_L by pipetting a solution to a lipid membrane within a traditional electrophysiology system, it was previously reported that full length BcL-x_L can disassemble C_{16}-ceramide channels formed in planar phospholipids membranes, strongly suggesting a direct interaction between Bcl-x_L and the ceramide channel.[45]

It is intriguing to explore the molecular mechanisms of such interactions, and one approach is the use of point mutations at critical sites. Here we explore reversible interactions between the Y101K mutant of Bcl-x_L and solitary ceramide channels. The Y101K mutant of wild type Bcl-x_L has a mutation of amino acid 101 from tyrosine to lysine, which blocks the ability of Bcl-x_L to heterodimerize with Bax. However, it retains the ability to prevent membrane permeabilization but with lower activity.[27] In this study, C_{16}-ceramide channels formed on a phospholipid membrane in the microfluidic chip were disassembled by Y101K. Upon the perfusion of Y101K to an on-chip membrane containing a single ceramide channel, the channel conductance was knocked down almost to zero, with the reduction occurring over a period of ~3 min in multiple steps. Similarly, when the Y101K solution was displaced by continuous perfusion with base salt buffer, the ceramide channel was observed to reassemble in as a series of stepwise conductance increments (Fig. 5) with individual steps occurring on time intervals of 3–5 min. These results suggest a direct but weak interaction between Y101K and the ceramide channel.

CONCLUSION

The microfluidic BLM system represents the first demonstration of a robust membrane model enabling effective kinetic studies of lipid ion channels. The system offers perfusion capabilities that are not feasible with traditional membrane models, allowing rapid changes in the solutes at the lipid membrane with arbitrary concentration profiles. Moreover, small sample consumption, less than 100 μL in a typical multiple-injection experiment, significantly reduces the cost for tests performed using precious materials such as expressed proteins.

The BLM platform has been applied to studies of ceramide, a biologically important channel-forming lipid whose kinetic interactions are not yet well understood. The results present a new view of the dynamic interactions between free ceramide molecules, ceramide channels, La^{3+} as a channel inhibitor, and EDTA as a chelator for reversal of the channel inhibition process. Using the microfluidic chip, both the kinetics and subconductance levels

involved in these interactions have been resolved. Similarly, we have demonstrated the utility of the microfluidic system to elucidate the kinetic features of reversible interactions between ceramide channels and the Y101K mutant of Bcl-x_L, a ligand known to be associated with ceramide channel inhibition. While further experiments are ongoing to understand the detailed behavior of ceramide channels observed in these measurements, the results presented here reveal the ability of the perfusion system to probe channel kinetics that would otherwise be inaccessible.

Application of the microfluidic technology is not limited to ceramide, but has broader implications for studies of protein ion channels, based on the emerging recognition that the regulation of ion channel function is modulated by the lipid membranes themselves. More generally, the platform opens the door to new opportunities for studying complex dynamic processes involved in membrane biophysics.

Acknowledgments

The authors gratefully acknowledge Dr. Louis Hromada for input on chip fabrication, Meenu Perera for assistance with pClamp software and Vidyaramanan Ganesan for providing the Bcl-x_L mutant. We thank Dr. David W. Andrews at McMaster University in Canada for providing plasmid for protein preparation. This work is supported by NIH grants R01GM072512 and R21EB011750.

REFERENCES

1. Anishkin A, Sukharev S, Colombini M. Searching for the molecular arrangement of transmembrane ceramide channels. Biophys. J. 2006; 90:2414–2426. [PubMed: 16415050]
2. Antonov VF, Petrov VV, Molnar AA, Predvoditelev DA, Ivanov AS. Appearance of single-ion channels in unmodified lipid bilayer-membranes at the phase-transition temperature. Nature. 1980; 283:585–586. [PubMed: 6153458]
3. Antonov VF, Smirnova EY, Shevchenko EV. Electric-field increases the phase-transition temperature in the bilayer-membrane of phosphatidic-acid. Chem. Phys. Lipids. 1990; 52:251–257. [PubMed: 2340602]
4. Bernardi P, Scorrano L, Colonna R, Petronilli V, Di Lisa F. Mitochondria and cell death—mechanistic aspects and methodological issues. Eur. J. Biochem. 1999; 264:687–701. [PubMed: 10491114]
5. Billen LP, Kokoski CL, Lovell JF, Leber B, Andrews DW. Bcl-XL inhibits membrane permeabilization by competing with Bax. PLoS Biol. 2008; 6:e147. [PubMed: 18547146]
6. Boheim G, Hanke W, Eibl H. Lipid phase-transition in planar bilayer-membrane and its effect on carrier-mediated and pore-mediated ion-transport. Proc. Natl Acad. Sci. Biol. 1980; 77:3403–3407.
7. Chen CF, Liu J, Hromada LP, Tsao CW, Chang CC, DeVoe DL. High-pressure needle interface for thermoplastic microfluidics. Lab Chip. 2009; 9:50–55. [PubMed: 19209335]
8. Cohen FS, Akabas MH, Zimmerberg J, Finkelstein A. Parameters affecting the fusion of unilamellar phospholipid vesicles with planar bilayer membranes. J. Cell Biol. 1984; 98:1054–1062. [PubMed: 6699081]
9. Cohen FS, Zimmerberg J, Finkelstein A. Fusion of phospholipid vesicles with planar phospholipid bilayer membranes. II. Incorporation of a vesicular membrane marker into the planar membrane. J. Gen. Physiol. 1980; 75:251–270. [PubMed: 6247418]
10. Colombini M. Ceramide channels and their role in mitochondria-mediated apoptosis. Biochim. Biophys. Acta. 2010; 1797:1239–1244. [PubMed: 20100454]
11. Crompton M. The mitochondrial permeability transition pore and its role in cell death. Biochem. J. 1999; 341:233–249. [PubMed: 10393078]
12. Dart C. Lipid microdomains and the regulation of ion channel function. J. Physiol. 2010; 588:3169–3178. [PubMed: 20519314]

13. Epshtein Y, Chopra AP, Rosenhouse-Dantsker A, Kowalsky GB, Logothetis DE, Levitan I. Identification of a C-terminus domain critical for the sensitivity of Kir2.1 to cholesterol. Proc. Natl Acad. Sci. USA. 2009; 106:8055–8060. [PubMed: 19416905]
14. Fantini J, Barrantes FJ. Sphingolipid/cholesterol regulation of neurotransmitter receptor conformation and function. Biochim. Biophys. Acta. 2009; 1788:2345–2361. [PubMed: 19733149]
15. Fertig N, Blick RH, Behrends JC. Whole cell patch clamp recording performed on a planar glass chip. Biophys. J. 2002; 82:3056–3062. [PubMed: 12023228]
16. Fertig N, Meyer C, Blick RH, Trautmann C, Behrends JC. Microstructured glass chip for ion-channel electrophysiology. Phys. Rev. E. 2001; 64 040901.
17. Funakoshi K, Suzuki H, Takeuchi S. Lipid bilayer formation by contacting monolayers in a microfluidic device for membrane protein analysis. Anal. Chem. 2006; 78:8169–8174. [PubMed: 17165804]
18. Ganesan V, Colombini M. Regulation of ceramide channels by Bcl-2 family proteins. FEBS Lett. 2010; 584:2128–2134. [PubMed: 20159016]
19. Ganesan V, Perera MN, Colombini D, Datskovskiy D, Chadha K, Colombini M. Ceramide and activated Bax act synergistically to permeabilize the mitochondrial outer membrane. Apoptosis. 2010; 15:553–562. [PubMed: 20101465]
20. Hausmann G, O'Reilly LA, van Driel R, Beaumont JG, Strasser A, Adams JM, Huang DC. Pro-apoptotic apoptosis protease-activating factor 1 (Apaf-1) has a cytoplasmic localization distinct from Bcl-2 or Bcl-x(L). J. Cell Biol. 2000; 149:623–634. [PubMed: 10791976]
21. Heimburg T. Lipid ion channels. Biophys. Chem. 2010; 150:2–22. [PubMed: 20385440]
22. Heimburg T, Jackson AD. The thermodynamics of general anesthesia. Biophys. J. 2007; 92:3159–3165. [PubMed: 17293400]
23. Holden MA, Bayley H. Direct introduction of single protein channels and pores into lipid bilayers. J. Am. Chem. Soc. 2005; 127:6502–6503. [PubMed: 15869249]
24. Holden MA, Jayasinghe L, Daltrop O, Mason A, Bayley H. Direct transfer of membrane proteins from bacteria to planar bilayers for rapid screening by single-channel recording. Nat. Chem. Biol. 2006; 2:314–318. [PubMed: 16680158]
25. Hromada LP, Nablo BJ, Kasianowicz JJ, Gaitan MA, DeVoe DL. Single molecule measurements within individual membrane-bound ion channels using a polymer-based bilayer lipid membrane chip. Lab Chip. 2008; 8:602–608. [PubMed: 18369516]
26. Hsu YT, Wolter KG, Youle RJ. Cytosol-to-membrane redistribution of Bax and Bcl-X(L) during apoptosis. Proc. Natl Acad. Sci. USA. 1997; 94:3668–3672. [PubMed: 9108035]
27. Jeong SY, Gaume B, Lee YJ, Hsu YT, Ryu SW, Yoon SH, Youle RJ. Bcl-x(L) sequesters its C-terminal membrane anchor in soluble, cytosolic homodimers. EMBO J. 2004; 23:2146–2155. [PubMed: 15131699]
28. Kasianowicz JJ, Brandin E, Branton D, Deamer DW. Characterization of individual polynucleotide molecules using a membrane channel. Proc. Natl Acad. Sci. USA. 1996; 93:13770–13773. [PubMed: 8943010]
29. Kaufmann K, Silman I. Proton-induced ion channels through lipid bilayer-membranes. Naturwissenschaften. 1983; 70:147–149. [PubMed: 6304539]
30. Kaufmann K, Silman I. The induction by protons of ion channels through lipid bilayer-membranes. Biophys. Chem. 1983; 18:89–99. [PubMed: 6313086]
31. Kroemer G, Dallaporta B, Resche-Rigon M. The mitochondrial death/life regulator in apoptosis and necrosis. Annu. Rev. Physiol. 1998; 60:619–642. [PubMed: 9558479]
32. Malmstadt N, Nash MA, Purnell RF, Schmidt JJ. Automated formation of lipid-bilayer membranes in a microfluidic device. Nano Lett. 2006; 6:1961–1965. [PubMed: 16968008]
33. Narula J, Pandey P, Arbustini E, Haider N, Narula N, Kolodgie FD, Dal Bello B, Semigran MJ, Bielsa-Masdeu A, Dec GW, Israels S, Ballester M, Virmani R, Saxena S, Kharbanda S. Apoptosis in heart failure: release of cytochrome c from mitochondria and activation of caspase-3 in human cardiomyopathy. Proc. Natl Acad. Sci. USA. 1999; 96:8144–8149. [PubMed: 10393962]

34. Papahadj D, Jacobson K, Nir S, Isac T. Phase-transitions in phospholipid vesicles—fluorescence polarization and permeability measurements concerning effect of temperature and cholesterol. Biochim. Biophys. Acta. 1973; 311:330–348. [PubMed: 4729825]
35. Patel HH, Murray F, Insel PA. Caveolae as organizers of pharmacologically relevant signal transduction molecules. Annu. Rev. Pharmacol. 2008; 48:359–391.
36. Sabra MC, Jorgensen K, Mouritsen OG. Lindane suppresses the lipid-bilayer permeability in the main transition region. Biochim. Biophys. Acta. 1996; 1282:85–92. [PubMed: 8679664]
37. Sandison ME, Morgan H. Rapid fabrication of polymer microfluidic systems for the production of artificial lipid bilayers. J. Micromech. Microeng. 2005; 15:S139–S144.
38. Sandison ME, Zagnoni M, Abu-Hantash M, Morgan H. Micromachined glass apertures for artificial lipid bilayer formation in a microfluidic system. J. Micromech. Microeng. 2007; 17:S189–S196.
39. Sandison ME, Zagnoni M, Morgan H. Air-exposure technique for the formation of artificial lipid bilayers in microsystems. Langmuir. 2007; 23:8277–8284. [PubMed: 17585789]
40. Schindler H. Formation of planar bilayers from artificial or native membrane vesicles. FEBS Lett. 1980; 122:77–79. [PubMed: 7194191]
41. Simons K, Ikonen E. Functional rafts in cell membranes. Nature. 1997; 387:569–572. [PubMed: 9177342]
42. Simons K, Toomre D. Lipid rafts and signal transduction. Nat. Rev. Mol. Cell Biol. 2000; 1:31–39. [PubMed: 11413487]
43. Siskind LJ, Colombini M. The lipids C-2- and C-16-ceramide form large stable channels—implications for apoptosis. J. Biol. Chem. 2000; 275:38640–38644. [PubMed: 11027675]
44. Siskind LJ, Davoody A, Lewin N, Marshall S, Colombini M. Enlargement and contracture of C-2-ceramide channels. Biophys. J. 2003; 85:1560–1575. [PubMed: 12944273]
45. Siskind LJ, Feinstein L, Yu TX, Davis JS, Jones D, Choi J, Zuckerman JE, Tan WZ, Hill RB, Hardwick JM, Colombini M. Anti-apoptotic Bcl-2 family proteins disassemble ceramide channels. J. Biol. Chem. 2008; 283:6622–6630. [PubMed: 18171672]
46. Siskind LJ, Fluss S, Bui M, Colombini M. Sphingosine forms channels in membranes that differ greatly from those formed by ceramide. J. Bioenerg. Biomembr. 2005; 37:227–236. [PubMed: 16167178]
47. Siskind LJ, Kolesnick RN, Colombini M. Ceramide channels increase the permeability of the mitochondrial outer membrane to small proteins. J. Biol. Chem. 2002; 277:26796–26803. [PubMed: 12006562]
48. Siskind LJ, Kolesnick RN, Colombini M. Ceramide forms channels in mitochondrial outer membranes at physiologically relevant concentrations. Mitochondrion. 2006; 6:118–125. [PubMed: 16713754]
49. Susin SA, Zamzami N, Kroemer G. Mitochondria as regulators of apoptosis: doubt no more. Biochim. Biophys. Acta. 1998; 1366:151–165. [PubMed: 9714783]
50. Suzuki H, Tabata K, Kato-Yamada Y, Noji H, Takeuchi S. Planar lipid bilayer reconstitution with a micro-fluidic system. Lab Chip. 2004; 4:502–505. [PubMed: 15472735]
51. Suzuki H, Tabata KV, Noji H, Takeuchi S. Highly reproducible method of planar lipid bilayer reconstitution in polymethyl methacrylate microfluidic chip. Langmuir. 2006; 22:1937–1942. [PubMed: 16460131]
52. Taylor G. Dispersion of soluble matter in solvent flowing slowly through a tube. Proc. R. Soc. Lond. A Math. Phys. Sci. 1953; 219:8.
53. Trauble H, Teubner M, Woolley P, Eibl H. Electrostatic interactions at charged lipid-membranes. 1. Effects of pH and univalent cations on membrane structure. Biophys. Chem. 1976; 4:319–342. [PubMed: 8167]
54. Urbankova E, Voltchenko A, Pohl P, Jezek P, Pohl EE. Transport kinetics of uncoupling proteins. Analysis of UCP1 reconstituted in planar lipid bilayers. J. Biol. Chem. 2003; 278:32497–32500. [PubMed: 12826670]
55. Wiesner DA, Kilkus JP, Gottschalk AR, Quintans J, Dawson G. Anti-immunoglobulin-induced apoptosis in WEHI 231 cells involves the slow formation of ceramide from sphingomyelin and is blocked by bcl-XL. J. Biol. Chem. 1997; 272:9868–9876. [PubMed: 9092523]

56. Woodbury DJ. Nystatin/ergosterol method for reconstituting ion channels into planar lipid bilayers. Meth. Enzymol. 1999; 294:319–339. [PubMed: 9916236]

57. Woodbury DJ, Miller C. Nystatin-induced liposome fusion. A versatile approach to ion channel reconstitution into planar bilayers. Biophys. J. 1990; 58:833–839. [PubMed: 1701101]

58. Woodbury DJ, Rognlien K. The t-SNARE syntaxin is sufficient for spontaneous fusion of synaptic vesicles to planar membranes. Cell Biol. Int. 2000; 24:809–818. [PubMed: 11067766]

59. Yafuso M, Kennedy SJ, Freeman AR. Spontaneous conductance changes, multilevel conductance states and negative differential resistance in oxidized cholesterol black lipid-membranes. J. Membr. Biol. 1974; 17:201–212. [PubMed: 4368004]

60. Yethon JA, Epand RF, Leber B, Epand RM, Andrews DW. Interaction with a membrane surface triggers a reversible conformational change in Bax normally associated with induction of apoptosis. J. Biol. Chem. 2003; 278:48935–48941. [PubMed: 14522999]

61. Zagnoni M, Sandison ME, Marius P, Lee AG, Morgan H. Controlled delivery of proteins into bilayer lipid membranes on chip. Lab Chip. 2007; 7:1176–1183. [PubMed: 17713617]

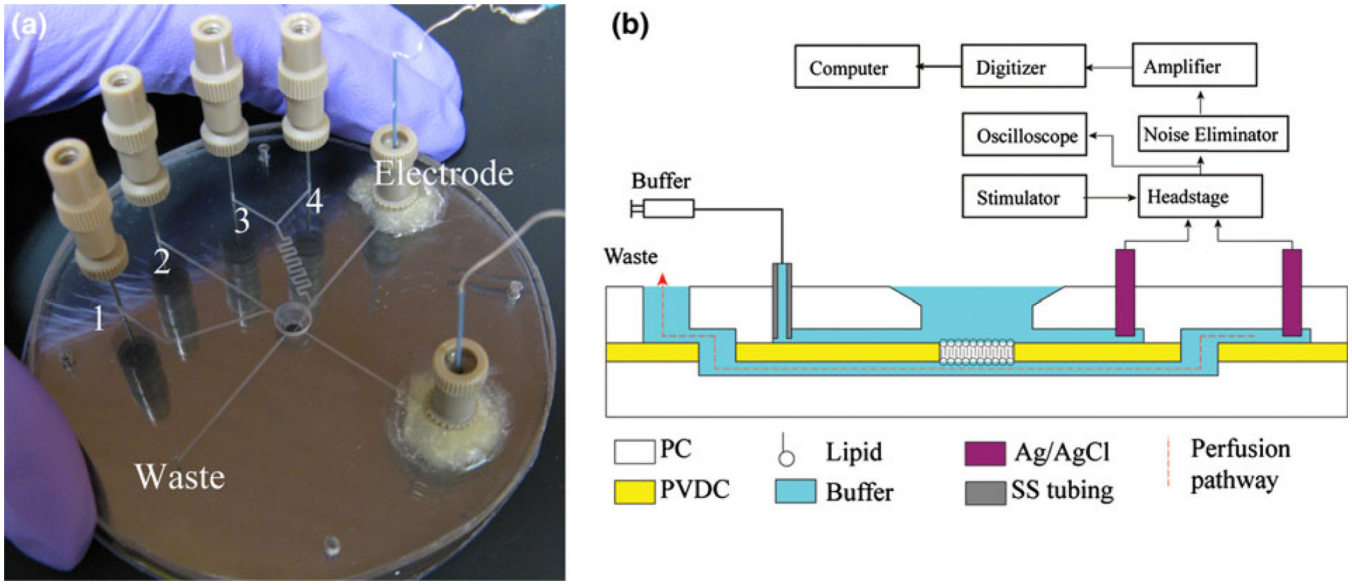

FIGURE 1.

(a) An assembled microfluidic perfusion chip. Buffer is introduced through a main channel on the top wafer (inlet 2), with an optional side channel (inlet 1) used to co-inject ion channels or other solutions to the open well. Two perfusion channels (inlets 3 and 4) connect to lower channel beneath the BLM site through a mixer. Two Ag/AgCl electrodes are sealed to chip with adhesive wax. (b) A cross-section schematic view of chip showing the electrical interface used for monitoring transmembrane current. The perfusion pathway (dashed line) passes beneath the BLM site to the waste port.

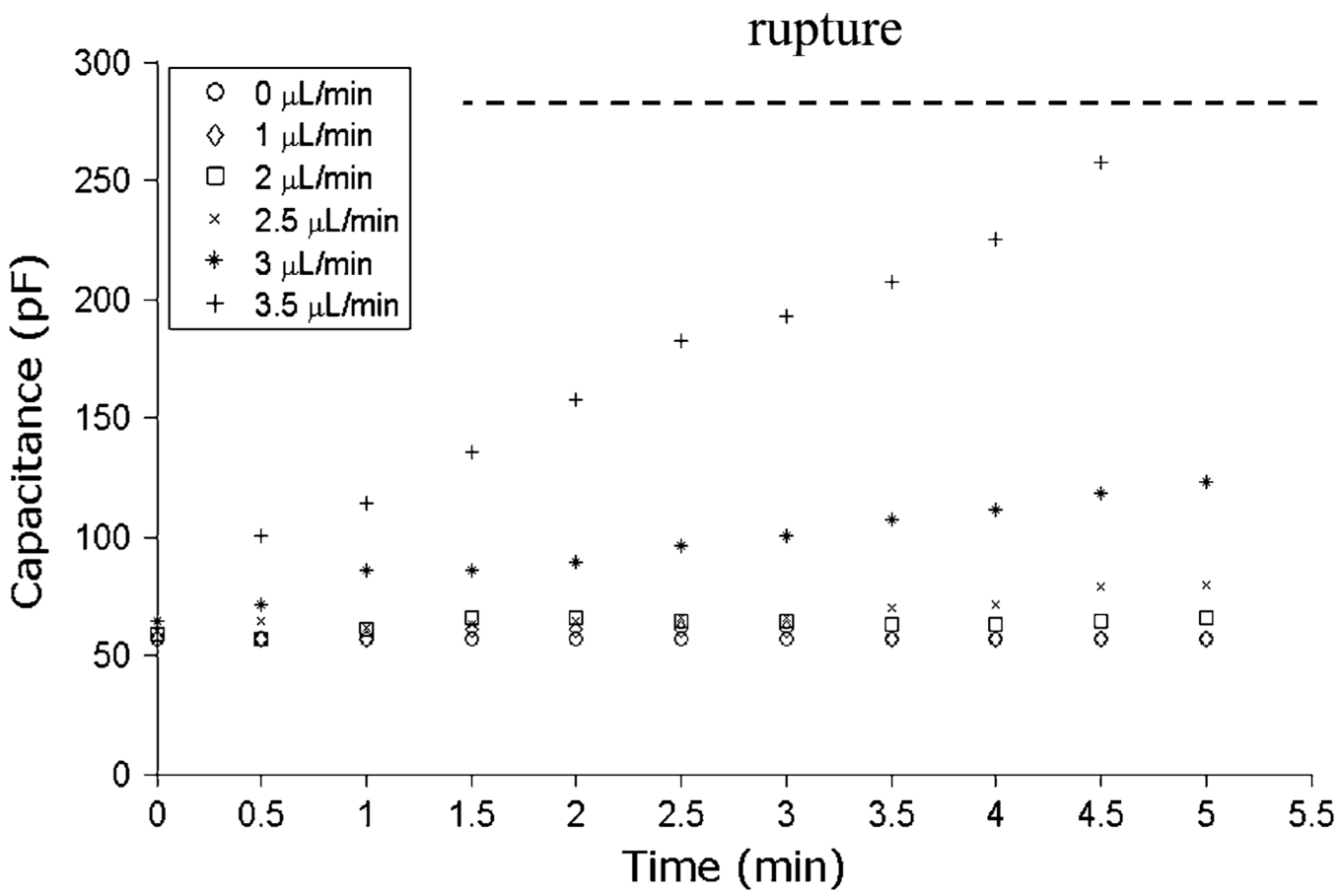

FIGURE 2.

Measurements of BLM capacitance over time at different perfusion flow rates up to 3.5 μL/min using a device with a 140 μm diameter membrane aperture. For flow rates up to 2.5 μL/min, negligible increases in membrane capacitance are observed, indicating that the membranes used in this study remain stable over this range. For higher flow rates, capacitance increases linearly with time, corresponding to an observed outward migration of the membrane boundary toward the aperture limits. Regardless of the flow rate, halting perfusion immediately returns the capacitance to its original state provided that the membrane has not been ruptured. At 3.5 μL/min, it takes approximately 5 min to reach the critical rupture point. For chips containing smaller apertures on the order of ~50 μm, maximum continuous pumping flow rates of 10 μL/min are routinely achieved.

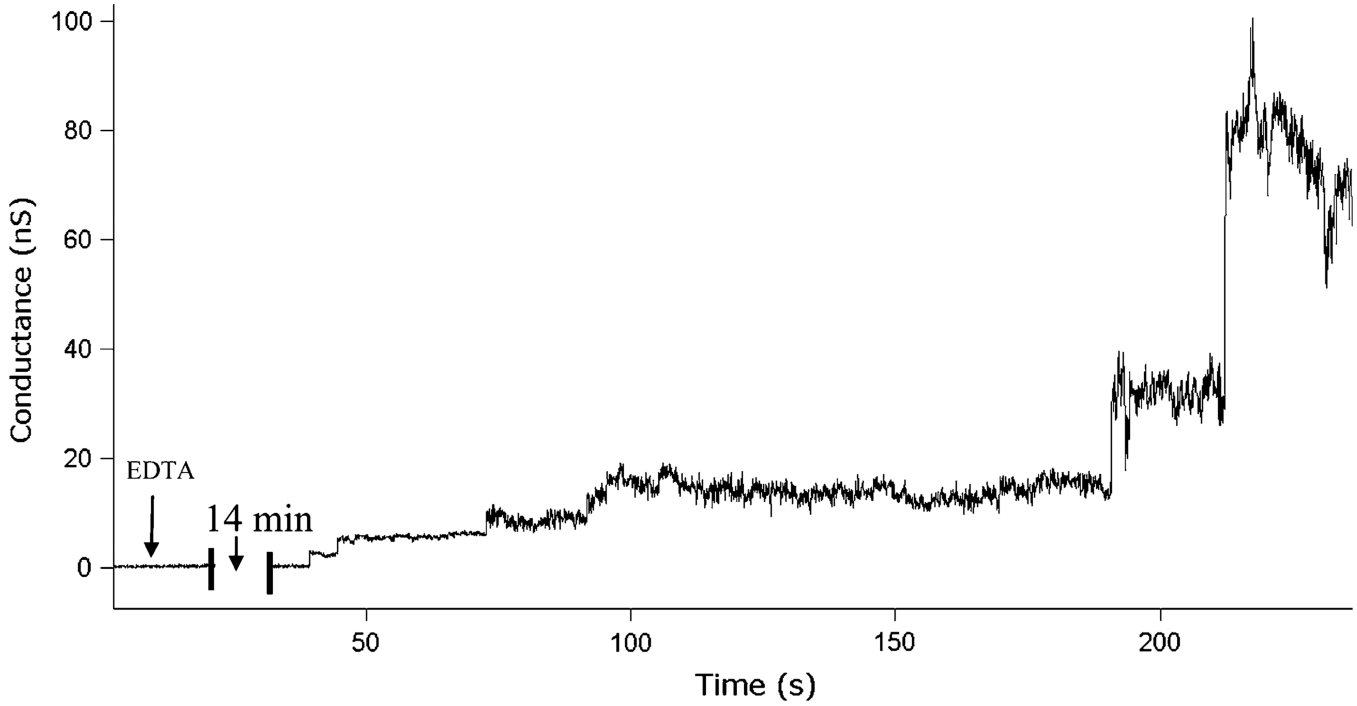

FIGURE 3.

Ceramide channel formation within a membrane pretreated with 50 μM $LaCl_3$ when 50 μM EDTA starts to be perfused to the membrane at time 0. At the given continuous perfusion flow rate (0.2 μL/min), EDTA first reaches the BLM site after an estimated 11.5 min period, followed by a switching time of τ = 72 s to reach the final concentration. Gradual stepwise channel formation is observed beginning 14 min after initiating EDTA perfusion (aperture diameter ~65 μm).

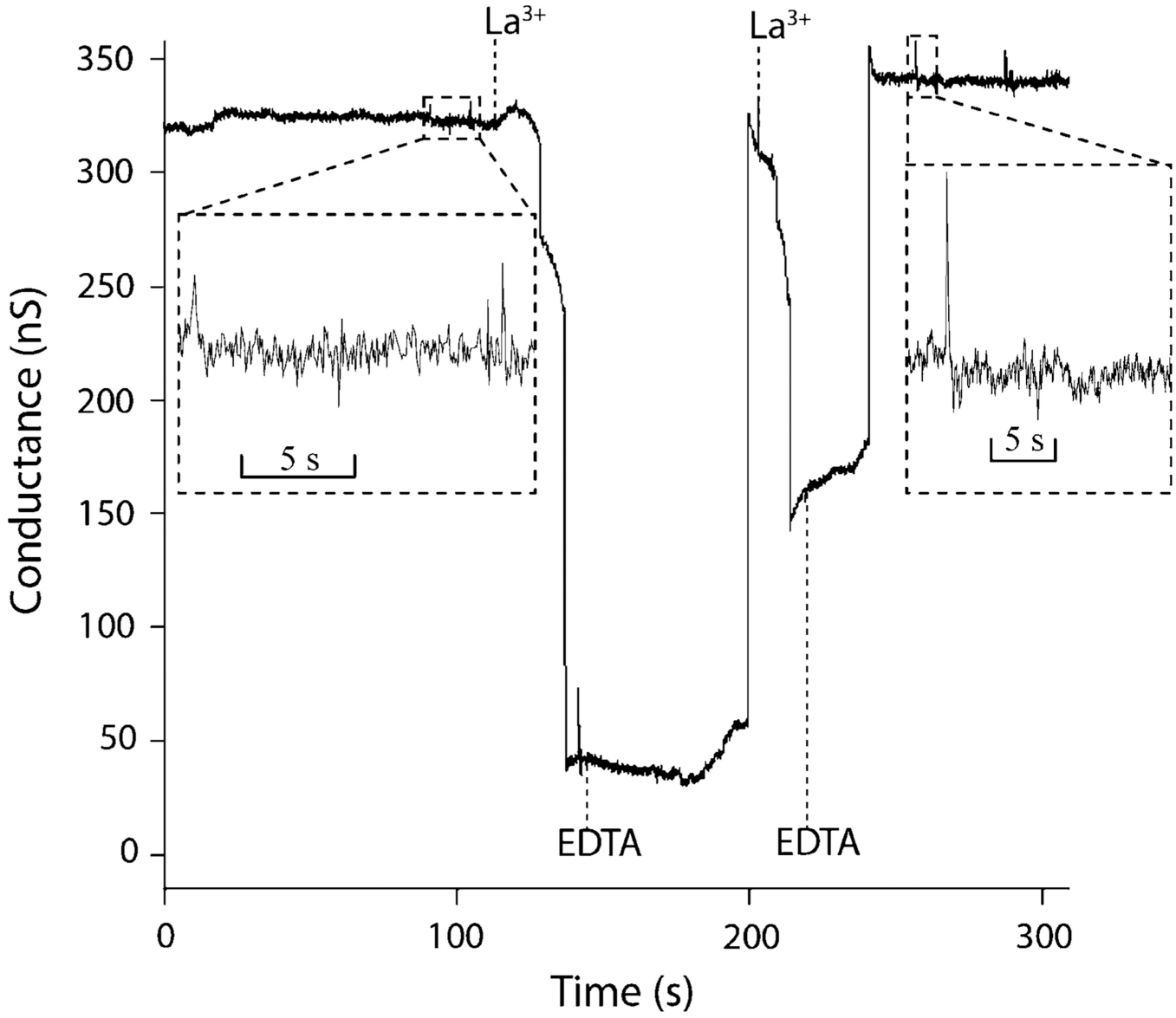

FIGURE 4.

Dynamic measurements of ceramide channel response to sequential perfusions of 50 μM $LaCl_3$ and 50 μM EDTA. A rapid pulse flow rate of 20 μL/min was used, with a corresponding switching time of $\tau = 5.8$ s (aperture diameter ~60 μm). The time interval between arrival and removal of each injection is estimated as 33.8 s for first $LaCl_3$, 57.9 s for first EDTA, and 16.2 s for second $LaCl_3$. The insets show the sub-second details of ceramide channel activity before and after two cycles of inhibition and recovery.

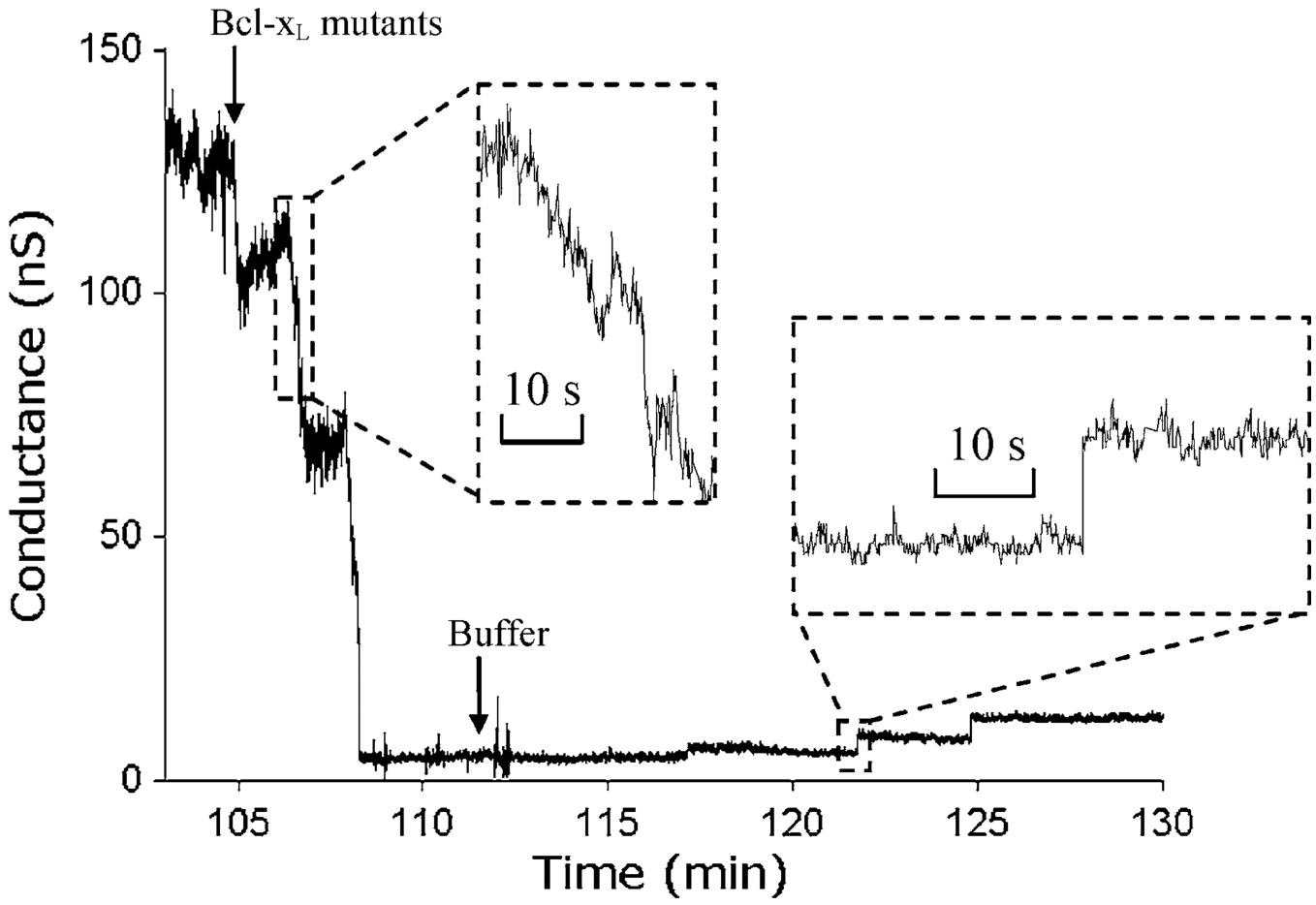

FIGURE 5.

A portion of 2-h current recording of ceramide interacting with Y101 Bcl-x_L mutants. The ceramide channel is initially stable at ~130 nS before perfusion of Bcl-x_L mutants with an estimated switching time of τ = 26.5 s at flow rate of 5 μL/min. The arrival of Bcl-x_L mutants (1.75 μg/mL) inhibits the ceramide channel conductance down to nearly zero over a 3 min period. Removal of Bcl-x_L from the BLM site by perfusion of buffer leads to slow stepwise recovery of the ceramide channel (aperture diameter ~70 μm). Inset shows a detailed view of stepwise channel disassembly and reassembly.